

Comparison of the Thermodynamics and Base-Pair Dynamics of a Full LNA:DNA Duplex and of the Isequential DNA:DNA Duplex[†]

Gilles Bruylants,[‡] Marina Bocconelli,[‡] Karim Snoussi,^{‡,#} and Kristin Bartik^{*.‡}

[‡]Molecular and Biomolecular Engineering, Service Matières et Matériaux, CP165/64, Université Libre de Bruxelles, 50 Avenue F.D. Roosevelt, 1050 Bruxelles, Belgium, and [#]Department of Chemistry, Université Catholique de Louvain, Bâtiment Lavoisier, Place Louis Pasteur, 1, B-1348 Louvain-la-Neuve, Belgium. [#]Current address: Japan Science and Technology Agency, NSEP Aoba Incubation Square, 468-15 Aramaki Aza Aoba, Aobaku, Sendai, Miyagi, 980-0845, Japan.

Received April 9, 2009; Revised Manuscript Received July 28, 2009

ABSTRACT: Locked nucleic acids (LNA), conformationally restricted nucleotide analogues, are known to enhance pairing stability and selectivity toward complementary strands. With the aim to contribute to a better understanding of the origin of these effects, the structure, thermal stability, hybridization thermodynamics, and base-pair dynamics of a full-LNA:DNA heteroduplex and of its isosequential DNA:DNA homoduplex were monitored and compared. CD measurements highlight differences in the duplex structures: the homoduplex and heteroduplex present B-type and A-type helical conformations, respectively. The pairing of the hybrid duplex is characterized, at all temperatures monitored (between 15 and 37 °C), by a larger stability constant but a less favorable enthalpic term. A major contribution to this thermodynamic profile emanates from the presence of a hairpin structure in the LNA single strand which contributes favorably to the entropy of interaction but leads to an enthalpy penalty upon duplex formation. The base-pair opening dynamics of both systems was monitored by NMR spectroscopy via imino protons exchange measurements. The measurements highlight that hybrid G-C base-pairs present a longer base-pair lifetime and higher stability than natural G-C base-pairs, but that an LNA substitution in an A-T base-pair does not have a favorable effect on the stability. The thermodynamic and dynamic data confirm a more favorable stacking of the bases in the hybrid duplex. This study emphasizes the complementarities between dynamic and thermodynamical studies for the elucidation of the relevant factors in binding events.

Locked nucleic acids (LNA),¹ conformationally restricted nucleotide analogues, constitute an important addition to the tools available for nucleic acid diagnostics and nucleic acid therapeutics. LNA monomers contain a modified ribose moiety in which the 2'O and 4'C are linked by a methylene bridge (2'-O,4'-C-methylene-β-D-ribofuranosyl), locking the sugar in the C3'-endo/N-type conformation (1–3). LNA resemble natural nucleic acids with respect to Watson–Crick base pairing and the potential of LNA containing oligonucleotides lies in their ability to mediate high affinity pairing with complementary RNA or DNA strands, with equal or often superior sequence specificity than their natural equivalent (4–7). Various applications and uses of LNA containing oligonucleotides have been reported and discussed in the literature. It has for example been shown that LNA containing oligonucleotides possess a gene silencing potential (7–9), that they are potential antisense drugs (10–12), and that they can be advantageously be used as probes in hybridization-based assays such as expression profiling,

DNA sequencing, and SNP genotyping (7, 13–19). It has furthermore been shown that the introduction of LNA monomers into DNA oligonucleotides ensures substantial serum stability, with low toxicity, which is a prerequisite for any potential therapeutic use (20).

Numerous structural and thermodynamic studies have been undertaken on LNA containing duplexes in order to try to elucidate the factors at the origin of the observed increased pairing selectivity and thermal stability. When LNA are incorporated into DNA or RNA:DNA duplexes they maintain a right-handed helix conformation with all the bases in the anti conformation. NMR studies however highlight that the incorporation of LNA monomers into DNA duplexes induces the local acquisition of A-type helix characteristics (21–26), with an increased N-type contribution to the sugar conformation of the DNA base-pairs adjacent to the incorporated LNA (23). The incorporation of LNA nucleotides into the DNA strand of a DNA:RNA hybrid duplex also leads to an increase in the deoxyribose N-type conformation (22, 26). When a full LNA strand is opposed to its cDNA strand the deoxyribose pucker pattern is similar to the one observed in RNA:DNA (24). These experimentally observed changes have been reproduced by Molecular Dynamic simulations (27, 28).

The stability of LNA-containing duplexes is generally evaluated via thermal denaturation experiments. The observed increase in the melting temperatures (T_m) of LNA containing duplexes relative to their native reference duplexes, range between +1 and

[†]G.B. thanks the Belgian “Fonds de la Recherche Scientifique – FNRS” for a postdoctoral fellowship. M.B. thanks the Belgian “Fonds pour la formation à la Recherche dans l’Industrie et dans l’Agriculture” for a Ph.D. grant.

*Corresponding author: Tel.: +32 6502063; fax: +32 6502606; e-mail: kbartik@ulb.ac.be.

[†]Abbreviations: LNA, locked nucleic acids; RNA, ribonucleic acid; DNA, deoxyribonucleic acid; DSC, differential scanning calorimetry; ITC, isothermal titration calorimetry; NMR, nuclear magnetic resonance; CD, circular dichroism.

+8 °C per LNA monomer introduced into a DNA strand paired to its cDNA strand (1, 20, 29–35) and between +2 and +9 °C when paired to its complementary RNA strand (1, 29–31, 36). The observed range of ΔT_m for each LNA nucleotide is however sequence dependent with both 5' and 3' unmodified neighbors influencing stability. The increase in T_m saturates for an approximate LNA content of 50% (4, 31). This has been interpreted as a consequence of the ability of LNA monomers to induce A-type characteristics, an effect which reaches a maximum when 50% of the nucleotides are modified (21, 23). The enthalpic (ΔH°) and entropic (ΔS°) contributions to the free energy (ΔG°) characterizing the stability of LNA containing duplexes have in a few cases been extracted from the thermal denaturation data (2, 29, 34–38). A more efficient stacking of the bases in LNA containing duplexes, resulting from the induced A-type helical conformation, is evoked for the origin of a more favorable enthalpic term (2, 34–36, 39). A more favorable entropic term is explained by the restriction of ribose flexibility and also by a favorable preorganization of the LNA containing single strands (2, 34, 39). The influence of LNA on the stability of 2'-O-methyl RNA/RNA duplexes has also been studied (39, 40), and there too enhanced stacking interactions and helical preorganization of the single-stranded oligonucleotides are reported as contributing to the stabilization of the duplexes.

When thermodynamic parameters are derived from the analysis of denaturation curves, they are obtained at T_m . As ΔH° and ΔS° can be strongly temperature dependent a comparison between duplexes is truly meaningful only if these quantities are extrapolated to a common temperature. This requires the knowledge of the ΔC_p of the systems, the difference between the molar heat capacity of the duplex and of the single strands parameter which can in principle be derived from DSC and UV data but rarely with good precision (41–43). A more precise and complete thermodynamic characterization of duplex formation can be obtained by isothermal titration calorimetry (ITC) which is able to provide, at any given temperature, the complete thermodynamic profile of a complexation process (ΔG° , ΔH° , and ΔS°). By performing experiments at different temperatures, it is also possible to obtain ΔC_p with good precision. To our knowledge, few studies reported in the literature take advantage of this technique to characterize the complexation between oligonucleotides (43–48), and only one reports data pertaining to the pairing of LNA/DNA strands to their complementary RNA strand (36).

With the aim to contribute to the understanding of the physicochemical principles underlying the remarkable properties of LNA, we used ITC to study the pairing thermodynamics of an 11 base-pair synthetic full-LNA:DNA duplex and of its isosequential DNA:DNA duplex. The thermal stability of the two systems was also monitored, for comparison reasons, by UV absorption spectroscopy and by DSC. The oligonucleotide was chosen as it has already been the subject of many structural studies. The natural duplex is known to form a full B-DNA type turn (49). Its sequence and length are furthermore particularly well adapted to physicochemical studies, including NMR studies (49, 50).

5'-CGCACACACGC-3' DNA 5'-CGCACACACGC-3' LNA

3'-GCGTGTGTGCG-5' DNA 3'-GCGTGTGTGCG-5' DNA

As LNA containing oligonucleotides have potential in various applications where base-pair opening is of utmost importance,

we also investigated the effect of LNA on base-pair opening dynamics by comparing, via NMR experiments, the exchange times of the imino protons of the hybrid duplex with those of the natural duplex. Proton exchange studies have been reported for different DNA duplex conformations (51–55), drug–DNA complexes (56), tRNA (57) and RNA duplexes (55, 58), but to our knowledge no data pertaining to the base-pair dynamics of LNA containing oligonucleotides have been reported in the literature.

MATERIALS AND METHODS

Preparation of Samples. The two cDNA strands and the LNA strand were purchased in the sodium salt form from Eurogentec (Belgium). The cytosines in the LNA strand are all methylated (5-Me-C-LNA). All batches were dialyzed previous to any use against a large volume of milli-Q H₂O with a MW cutoff of 1 kDa. Pairing of the strands was achieved by heating a solution containing an equal number of moles of each strand to 95 °C for 10 min and then letting the system cool slowly. The obtained duplex was dialyzed against a large volume of milli-Q H₂O with a MW cutoff of 3.5 kDa and lyophilized before dilution in the desired buffer. The oligonucleotide concentrations were determined spectrophotometrically by measuring the absorbance at room temperature at 260 nm and using $\epsilon = 99\,600\text{ M}^{-1}\text{ cm}^{-1}$ for the strand 5'-CGCACACACGC-3' called strand A, $\epsilon = 101\,300\text{ M}^{-1}\text{ cm}^{-1}$ for the strand 5'-GCGTGTGTGCG-3' called strand T and $\epsilon = 168\,200\text{ M}^{-1}\text{ cm}^{-1}$ for the duplexes. The ϵ value of the DNA:DNA duplex was previously determined in our laboratory (details given in ref 59). The ϵ values for the single strands were obtained using the nearest neighbor model and its published parameters for DNA at room temperature (60). The coefficients used for the LNA single strand and the hybrid duplex were the same as those used for the homologous DNA systems. The change with temperature (between 5° and 60 °C) of the ϵ values of the single strands at 260 nm was less than 2%.

A pH=7, 10 mM sodium phosphate buffer with 100 mM NaCl and 0.1 mM EDTA, was used for the thermal denaturation (UV, DSC, NMR), CD and ITC experiments.

UV Melting experiments were carried out with a Perkin-Elmer lambda-40 spectrophotometer equipped with a PTP-1 DNA melting kit. Absorbance vs temperature curves were measured using a heating rate of 1 K/min. The temperature was measured directly in the sample using a thermocouple adapted to the cell cap. The absorbance was measured, depending on sample concentration, at either 260 or 290 nm and using either a 10 mm or a 2 mm path length. Concentrations ranged between 1 μM and 100 μM for the duplexes and between 5 μM and 20 μM for the single strands. The T_m and $\Delta H^\circ(T_m)$ were derived from the denaturation curves using the well described “two-state” model (50, 61) where the absorbance is expressed as a function of α , the fraction of strands in the single strand form, A_{ds} , the absorbance of the solution containing only the duplex and A_{ss} , the absorbance of the solution containing only single strand oligonucleotides (eq 1):

$$A_{\text{obs}} = (1 - \alpha)A_{ds} + \alpha A_{ss} \quad (1)$$

An expression for α can be extracted from eq 2 (where C_0 is the total concentration of each strand) and inserted into eq 1 which can then be fitted to the experimental melting curve

186 treating ΔH° , T_m , and the parameters describing the linear
 187 variation of A_{ds} and A_{ss} with temperature as variable para-
 188 meters.

$$\frac{\alpha^2 C_0^2}{C_0(1-\alpha)} = \exp\left(-\frac{\Delta H^\circ}{R}\left(\frac{1}{T} - \frac{1}{T_m}\right) + \ln \frac{C_0}{2}\right) \quad (2)$$

189 At least five runs were performed for each sample and
 190 reported errors correspond to the 95% confidence interval.

191 *DSC experiments* were carried out using a scan rate of 1 K/min
 192 with a Calorimetric Science Corporation nanoDSC-II differen-
 193 tial adiabatic scanning microcalorimeter equipped with 0.3268
 194 mL cells. Integration of the area between the C_p versus T curve
 195 and the baseline, constructed using the two-state model, yields
 196 the transition enthalpy ($\Delta H^\circ(T_m)$) and T_m is the temperature
 197 which divides this area in two. All data were processed using the
 198 standard CSC software. Concentrations ranged between 25 and
 199 100 μM for the duplexes and experiments were run on the single
 200 strands at a concentration of approximately 200 μM . At least five
 201 runs were performed for each sample, and reported errors
 202 correspond to the 95% confidence interval.

203 *ITC experiments* were performed on an ITC-4200 from
 204 Calorimetric Science Corporation. Aliquots of 5 μL of a solution
 205 of one of the strands of a known precise concentration (in the
 206 250 μM range) were injected into the 1.3 mL titration cell
 207 containing the solution of the complementary strand (in the
 208 10 μM range). Twenty injections were typically performed for
 209 each set of experimental conditions at intervals of 600 s to ensure
 210 the return to equilibrium. Blank experiments were performed in
 211 order to take ligand dilution heat into consideration (heat
 212 removed before analyzing the titration data). Fitting of a 1:1
 213 binding model to the experimental data was undertaken with
 214 program developed in-house, using a simplex algorithm to
 215 minimize a cost function which takes into account the errors
 216 on (i) the heat exchanges after each injection (at least three
 217 individual baselines were constructed in order to estimate an
 218 error on the individual Q_i) and on (ii) the concentrations in the
 219 cell (linked to errors on ϵ and on the volume of injection). The
 220 heat of the first injection was systematically removed for analysis.

221 *CD spectra* were recorded at room temperature for both
 222 duplexes at a concentration of 140 and 75 μM for the LNA:
 223 DNA and DNA:DNA duplexes, respectively, on a JASCO J-710
 224 CD spectrometer with a 0.02 cm cell. Each CD spectrum was the
 225 accumulation of eight scans recorded at 50 nm/min with a 1 nm
 226 slit and a time constant of 0.5 s for a nominal resolution of
 227 0.5 nm. Data were collected from 200 to 320 nm.

228 *One dimensional ^1H NMR* experiments were acquired, at
 229 different temperatures, on a Varian Unity - 600 MHz spectro-
 230 meter using the jump-return pulse sequence with a delay which
 231 maximizes the imino proton intensities (50 μs) (62). Spectra were
 232 recorded with a minimum of 512 transients, an acquisition time
 233 of 2 s, a recycle delay of 2 s, a spectral width of 12000 Hz, and a
 234 digital resolution of at least 0.5 Hz/pt. The FIDs were weighted
 235 by a 2 Hz exponential multiplication prior to Fourier transfor-
 236 mation. Concentrations of the single strands and of the duplexes
 237 were approximately 200 μM .

238 The assignment of the signals of the DNA:DNA duplex has
 239 been previously reported (49) and the assignment of the DNA:
 240 LNA imino protons was achieved by 2D NOESY spectra
 241 collected with mixing times ranging from 100 to 300 ms.

242 Imino proton exchange experiments were performed at 20 and
 243 15 $^\circ\text{C}$ using NH_3 as proton acceptor. The formalism of catalyzed

Table 1: T_m Derived from UV and DSC Thermal Denaturation Experi-
 ments for Different Concentrations of the DNA:DNA and LNA:DNA
 Duplexes^a

[db] (μM)	T_m ($^\circ\text{C}$)	
	DNA:DNA	LNA:DNA
100	68 \pm 1	102 \pm 2
50	64 \pm 2	99 \pm 2
25	62 \pm 1	97 \pm 2
1	54 \pm 1	

^aFor the DNA:DNA duplex the value correspond to the mean of the
 UV and DSC experiments while for LNA only DSC gave appropriate
 results.

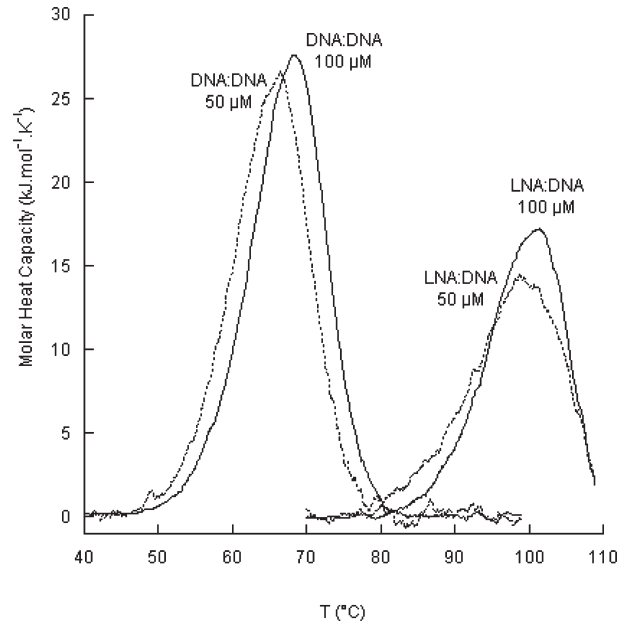


FIGURE 1: DSC thermograms (molar heat capacity) of the DNA:
 DNA and LNA:DNA duplexes at two different concentrations.

244 imino proton exchange is described in the literature (63). Imino
 245 protons exchange with water from the transiently open state via
 246 an acid–base reaction catalyzed by proton acceptors. The proton
 247 acceptor contribution to the exchange time is given by

$$\tau_{\text{ex,cat}} = \tau_{\text{cl}} + \frac{1 + 10^{\text{p}K(\text{nu}) - \text{p}K(\text{acc})}}{\alpha k_{\text{coll}} K_d [\text{acc}]} \quad (3)$$

248 where τ_{cl} is the base-pair lifetime, K_d is the base-pair dissociation
 249 constant ($\tau_{\text{op}}/\tau_{\text{cl}}$), k_{coll} is the collision rate (considered here to be
 250 equal 10^9 s^{-1}) (63), $\text{p}K(\text{nu})$ is the $\text{p}K$ of the monitored nucleotide
 251 imino proton (9.3 for G and 10.3 for T) (54), $\text{p}K(\text{acc})$ is the $\text{p}K$ of
 252 the proton acceptor, ($\text{p}K(\text{NH}_3) = 9.3$), $[\text{acc}]$ is the proton acceptor
 253 concentration and α is the accessibility factor of the proton
 254 acceptor for the imino protons in the open state (considered equal
 255 to 1 when NH_3 is used as proton acceptor) (63). The exchange
 256 contribution of the catalyst, $\tau_{\text{ex,cat}}$, was determined from the
 257 exchange times measured in the presence (τ_{ex}) and in the absence
 258 ($\tau_{\text{ex},0}$) of ammonia:

$$\tau_{\text{ex,cat}} = \left(\frac{1}{\tau_{\text{ex}}} - \frac{1}{\tau_{\text{ex},0}} \right)^{-1} \quad (4)$$

259 The plot of $\tau_{\text{ex,cat}}$ versus the inverse of catalyst concentration
 260 yields τ_{cl} and the dissociation constant.

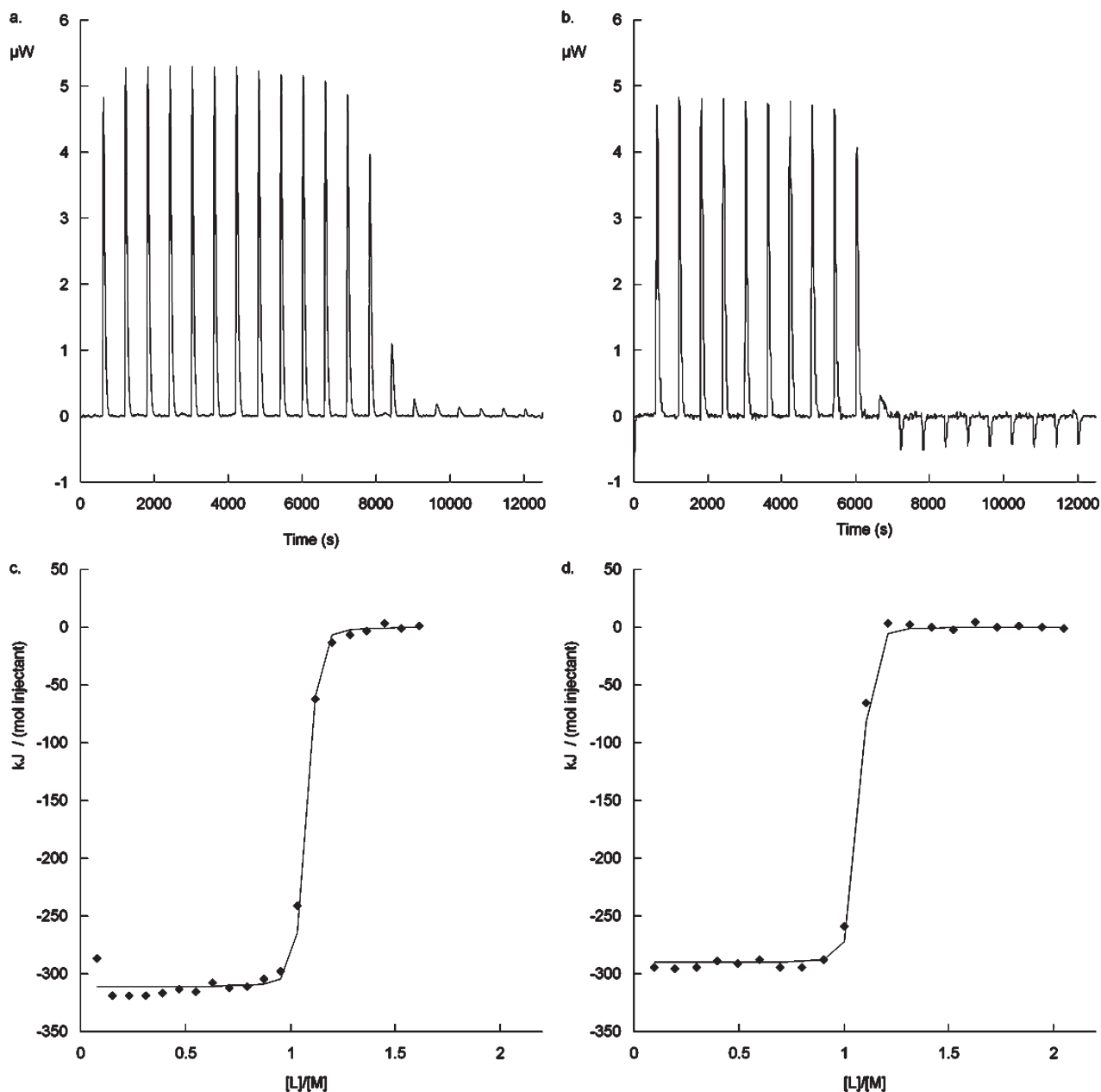


FIGURE 2: ITC titration profiles (upper panels) at 37 °C and enthalpies (lower panels) for the formation of the (A) DNA:DNA duplex and (B) LNA:DNA duplex. Blank experiments were run for all experiments to remove heats of dilution. The solid lines in the lower panels correspond to a 1:1 binding fit. The first data point was omitted from the fitting procedure. Concentration of DNA strand T in the cell was 10 μM for both titrations and the concentrations of ligand in the syringe were 200 and 230 μM for the DNA and LNA experiments, respectively.

261 Samples of lyophilized duplex were dissolved at a concentra- 277
 262 tion in the 500 μM range in a 90% H₂O/10% D₂O solution 278
 263 containing 1 mM EDTA. The pH was adjusted to 8.9 using 279
 264 concentrated solutions of NaOH and HCl. Aliquots of 6.5 M 280
 265 NH₄Cl were added to the initial solution to increase the catalyst 281
 266 concentration and the pH readjusted to 8.9 after each addition. 282

267 Exchange times were determined by magnetization transfer 283
 268 from water (63). Water magnetization was inverted using a 284
 269 DANTE sequence of six 30° hard pulses separated by 100 μs 285
 270 intervals. The residual transverse component was destroyed by a
 271 Z gradient (23 G/cm) applied after the DANTE sequence (500 μs)
 272 and a Z-gradient (0.01 G/cm) was also applied during the
 273 magnetization transfer delay (δ) to reduce radiation damping.
 274 The signal was detected using an echo water suppression
 275 subsequence with a 50 μs delay which maximizes the imino
 276 proton intensities (64). A 300 μs gradient was applied before

277 recording the FID (15 G/cm). A recovery delay of 15 s was used 278
 279 in order to allow full relaxation of the water magnetization. The 280
 281 imino proton exchange times at different catalyst concentrations 282
 283 were obtained using a minimum of 23 time increments and by 284
 285 fitting eq 3 to the experimental data. The delay never exceeded 286
 150 ms in order to avoid unwanted cross-relaxation effects. The
 longitudinal relaxation times of water (R_{1,w}) and of the imino
 protons (R_{1,i}) were determined with separate inversion–recovery
 experiments using a minimum of 11 time increments.

RESULTS AND DISCUSSION 286

287 *Stability of the Duplexes.* The thermal denaturation of 288
 289 the 11 base-pair DNA:DNA duplex was monitored by 290
 291 UV-spectroscopy and by DSC for duplex concentrations 292
 ranging between 1 μM and 100 μM. The T_m of the LNA:
 DNA duplex was too high, even at 1 μM, to be determined by

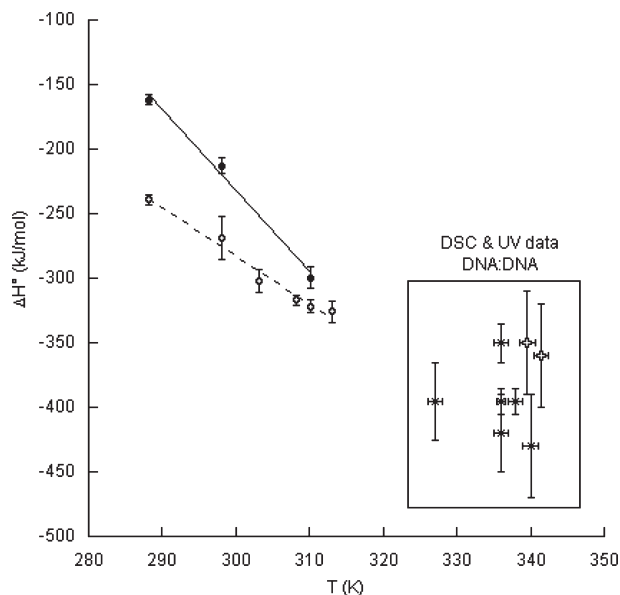


FIGURE 3: Enthalpies of formation (ΔH°) for the DNA:DNA (open circles) and the LNA:DNA (filled circles) duplexes as a function of temperature. The data obtained by UV and DSC are highlighted. The lines represent the linear weighted least-squares fits to the DNA:DNA (dashed line) and LNA:DNA (solid line) ITC data. The derived ΔC_p are $3.7 \pm 0.3 \text{ kJ mol}^{-1} \text{ K}^{-1}$ and $6.3 \pm 0.6 \text{ kJ mol}^{-1} \text{ K}^{-1}$ for the DNA:DNA and LNA:DNA duplexes, respectively.

UV-spectroscopy. It could however be estimated by DSC as it is possible to heat the sample to temperatures slightly above 100 °C in a DSC cell (pressurized at 3 atm). The T_m values obtained for the natural and hybrid duplexes at similar concentrations are reported in Table 1 and DSC thermograms are shown in Figure 1. The T_m of the LNA:DNA duplex are approximately 35 °C higher than those of the DNA:DNA duplex. These results are comparable to results reported in the literature for LNA:DNA duplexes studied under similar experimental conditions (2, 10, 24, 32, 33, 65).

The thermodynamic parameters pertaining to the pairing of the strands of the DNA:DNA and LNA:DNA duplexes were obtained by isothermal titration calorimetry (ITC) at temperatures between 15 and 37 °C. Figure 2 shows ITC data acquired at 37 °C for the titration of DNA strand A or LNA strand A into the cell containing the cDNA strand T (for all ITC results see Supporting Information). The heats of dilution of the single strands were taken into consideration when analyzing the data. They were found to be constant throughout the blank experiment and furthermore identical to the heat generated by the last injections in the pairing experiments. This indicates that there is no change in the aggregation states of the single strands. The parametric adjustment of the 1:1 binding model to the experimental data converges toward a larger value for the affinity constant for the LNA:DNA duplex, but as these K_a are very large and cannot be determined with precision, the data should only be considered qualitatively. Figure 3 shows the ITC determined ΔH° for both systems as a function of temperature. The $\Delta H^\circ(T_m)$ of the DNA:DNA duplex extracted from the UV and DSC data are also shown for comparison. At all temperatures, ΔH° is less favorable for the formation of the LNA:DNA duplex than for that of the DNA:DNA duplex. As the LNA:DNA duplex is more stable than the DNA:DNA duplex, the entropic contribution ($T\Delta S^\circ$) to duplex formation must consequently be less unfavorable for the LNA:DNA duplex.

The ^1H NMR spectra of the LNA single strand highlights that this strand adopts some structure at temperatures below 35 °C (see Supporting Information). Two imino proton signals are observed in the zone corresponding to the presence of H-bonds between correctly matched base-pairs. They are observed for high (200 μM) and low concentration (20 μM) solutions suggesting the presence of a monomolecular structure. The thermal monitoring of the LNA by UV highlights a melting transition with a T_m of 20 °C (concentrations between 5 and 20 μM) and characterized by a $\Delta H^\circ(T_m)$ of $-160 \pm 40 \text{ kJ/mol}$ (see Supporting Information). The denaturing of both DNA single strands did not exhibit a UV transition, and none of the strands exhibited a transition in the DSC scans.

The contribution of single strand order to the thermodynamics of duplex formation has been discussed in the literature (44, 48, 66, 67) where it has clearly been shown that the initial state of the single strands can make an important contribution to the thermodynamic profile of duplex formation. The presence of structure in the LNA single strand will lead to a lower entropic penalty upon the formation of the hybrid duplex at lower temperatures, such as those monitored by ITC. This entropic gain will not be present at higher temperatures, such as those monitored by thermal denaturing experiments, as the single strand is no longer structured. The fact that the sugar moieties in the LNA single strand are blocked in a particular conformation will of course contribute, at all temperatures, to a difference in the ΔS° of interaction of the two duplexes.

As the structuring of the LNA single strand is not a favorable helical preorganization, the disruption of the intrastrand hydrogen bonds will contribute in an unfavorable way to enthalpy of formation of the hybrid duplex at lower temperatures. At temperatures close to the T_m of the LNA single strand (293 K), the ΔH° characterizing duplex formation is $\sim 70 \text{ kJ/mol}$ less favorable for the hybrid duplex compared to the natural one. If the ΔH° of the LNA single strand is taken into account ($\sim 160 \text{ kJ/mol}$), it is clear that at these temperatures, the enthalpy that characterizes the interaction between the two strands in the hybrid duplex is significantly more favorable than the one characterizing the interaction between the two DNA strands in the natural duplex. This clearly suggests that, as previously mentioned (35, 36), enhanced stacking interactions exist in LNA containing duplexes due to their more A-type helical structure. CD spectra of the DNA:DNA and LNA:DNA duplex clearly highlight that the former adopts a B-type helical structure (one positive ($\sim 280 \text{ nm}$) and two negative, (~ 250 and $\sim 210 \text{ nm}$) peaks of approximately same intensity), while the latter adopts a RNA A-type helical structure (a maximum around 260 nm, a small negative peak around 240 nm, an intense negative peak around 210 nm and a slightly negative CD between 280 and 310 nm) (68). It is also possible that the methyl groups present on the LNA cytosines lead to more favorable London interaction in the hybrid duplex (69).

Analysis of the ITC data clearly shows that the ΔH° of both duplexes are temperature dependent. The slopes of the linear regressions performed on the ITC data (lines shown in Figure 3) yield ΔC_p values of $-3.7 \pm 0.3 \text{ kJ mol}^{-1} \text{ K}^{-1}$ and $-6.3 \pm 0.6 \text{ kJ mol}^{-1} \text{ K}^{-1}$ for the DNA:DNA and LNA:DNA duplexes, respectively. These values are obtained with a much greater accuracy and precision than the ones that can be derived from thermal denaturation studies. It is indeed impossible to estimate a ΔC_p with good precision from the concentration dependence of the $\Delta H^\circ(T_m)$ determined by UV and DSC, not only because the

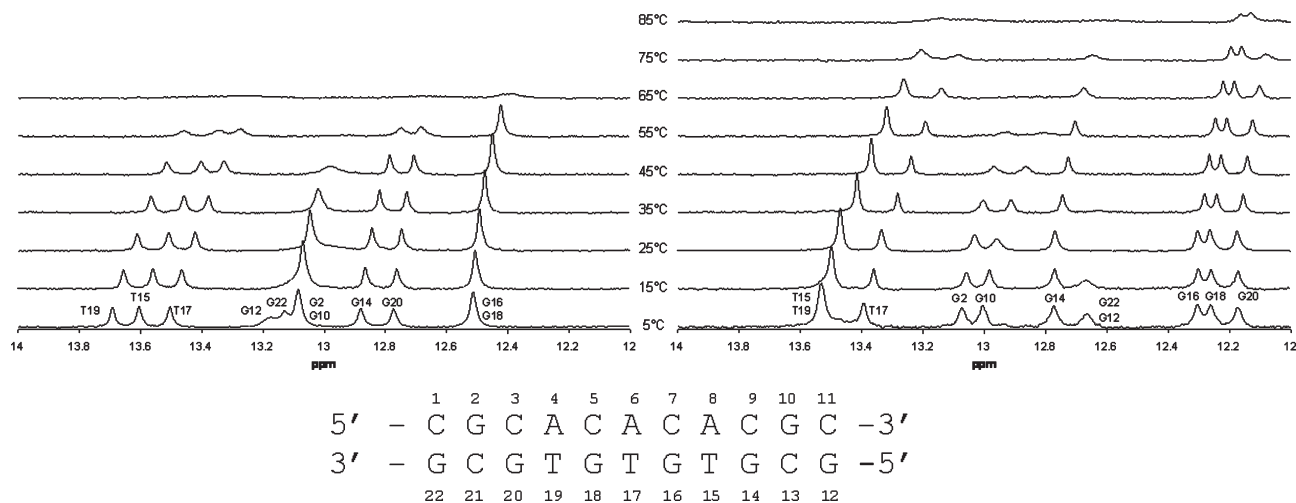


FIGURE 4: Imino signals of the (a) DNA:DNA and (b) LNA:DNA duplexes as a function of temperature. Peaks assignments are indicated on the spectra recorded at 5 °C.

389 temperature range is usually extremely narrow but also because
 390 of the scatter and large experimental errors associated with ΔH°
 391 values derived from denaturation curves. Regarding the possi-
 392 bility of determining $\Delta C_p(T_m)$ by measuring the difference, at T_m ,
 393 between the pre- and post-transitional baselines of a DSC
 394 thermogram, it is known that ΔC_p determined in this way are
 395 highly dependent on the choice of baselines – small perturbations
 396 in the regions assigned to the baseline can produce large changes
 397 in the ΔC_p (41–43).

398 No data on ΔC_p of LNA containing oligonucleotides have
 399 to our knowledge been reported in the literature. ITC derived
 400 values for various long DNA and RNA polynucleotides seem
 401 to indicate that their ΔC_p are essentially independent of
 402 sequence and of the nature of the nucleotide (DNA or RNA).
 403 An average value of $268 \pm 33 \text{ J mol}^{-1} \text{ K}^{-1}$ per base-pair has
 404 been reported (41). The ITC determined ΔC_p reported for
 405 shorter systems exhibit some variation with sequence and
 406 length (45–48, 70) with values for DNA:DNA and RNA:
 407 DNA duplexes, ranging between $-1.42 \text{ kJ mol}^{-1} \text{ K}^{-1}$ (47) and
 408 $-5.43 \text{ kJ mol}^{-1} \text{ K}^{-1}$ (48). Differences are observed in the ΔC_p
 409 of homologous DNA:DNA and RNA:DNA duplexes but with
 410 no systematic deviation (47, 70). The value determined in this
 411 study for the DNA:DNA duplex falls in the range of the ones
 412 reported in the literature for duplexes of similar length, while
 413 the value determined for the LNA:DNA duplex is somewhat
 414 higher.

415 An explanation for the molecular origin of the large negative
 416 ΔC_p of duplex formation is temperature-dependent changes in
 417 the thermodynamic state of the single strands (42, 43, 46, 48). The
 418 larger ΔC_p observed for the LNA:DNA duplex is most certainly
 419 the consequence of the fact that the LNA single strand adopts
 420 some structure at temperatures below 35 °C. In the higher
 421 temperature range sampled by thermal scanning methods, single
 422 strands are always essentially random coil and the ΔC_p measured
 423 via these methods will consequently not be influenced by an
 424 eventual coupled temperature-dependent equilibrium related to
 425 the single strands. The line drawn through the ITC determined
 426 ΔH° values reported in Figure 3 and whose slope yields the ΔC_p
 427 value can consequently not be extrapolated to higher tempera-
 428 tures. It can be expected that at higher temperatures the
 429 difference in the ΔC_p of the hybrid and natural duplex will
 430 essentially disappear.

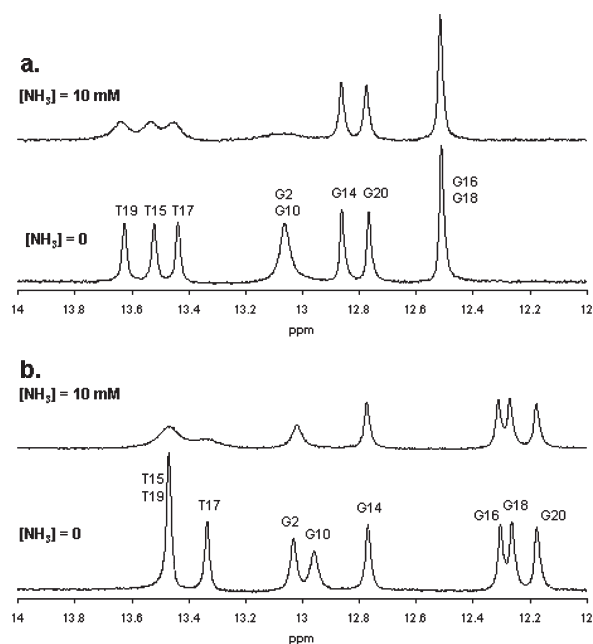


FIGURE 5: Imino signals of the (a) DNA:DNA and (b) LNA:DNA duplexes at 25 °C in the absence (lower spectra) and in the presence of approximately 10 mM NH_3 (upper spectra).

431 *Base-Pair Opening Dynamics.* The imino proton region in
 432 the ^1H NMR spectra of the DNA:DNA and LNA:DNA
 433 duplexes are shown in Figure 4 as a function of temperature
 434 with assignments indicated in the lowest temperature spectra.
 435 The signal intensities of the imino protons of both duplexes
 436 decrease with temperature as a consequence of their exchange
 437 with water protons. Exchange takes place when the hydrogen
 438 bond in which the imino proton is implicated is broken and
 439 when the lifetime of the open state is sufficient for proton
 440 transfer to occur (51). The exchange process, characterized by
 441 the rate constant k_{ex} , is consequently a function of the base-
 442 pair lifetime (τ_{cl}), the lifetime of the open state (τ_{op}), and
 443 the rate of transfer of the imino proton from the nucleoside to
 444 the proton acceptor (k_{tr}). These lifetimes and rate constants
 445 are temperature dependent and are furthermore different for each
 446 imino proton which explains why the different signals in the ^1H
 447 spectrum do not all disappear at the same temperature (51,
 448 71–73).

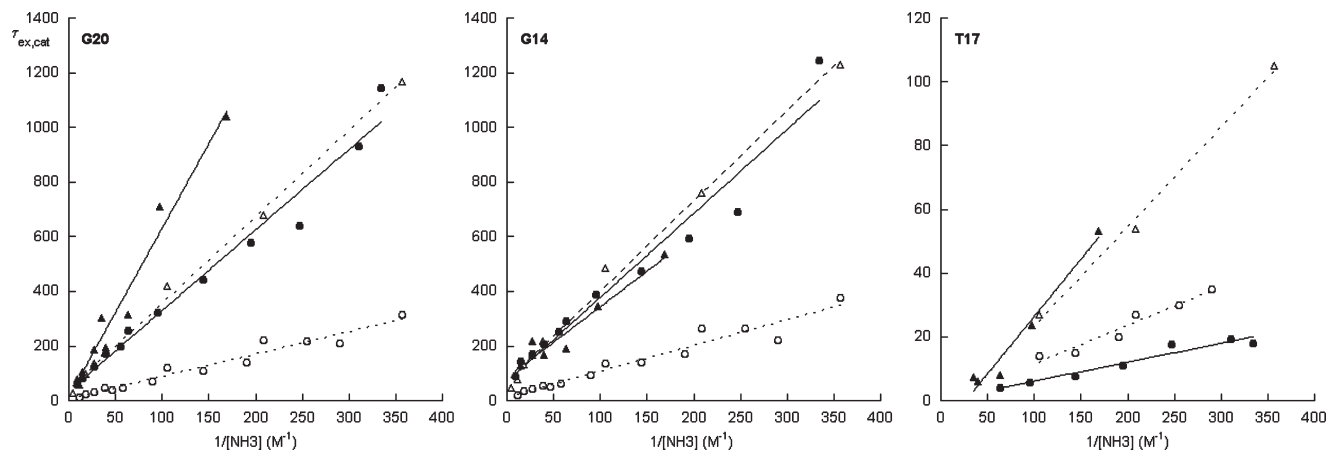


FIGURE 6: Proton acceptor contribution at 25 °C (circles) and 15 °C (triangles) for the (a) G20, (b) G14, and (c) T17 imino exchange times as a function of the inverse of the proton acceptor concentration. Filled symbols and full lines relate to the LNA:DNA duplex and open symbols and dashed lines relate to the DNA:DNA duplex. Lines correspond to a least-squares linear adjustment of eq 1 to the experimental data points.

449 In both duplexes the first signals to disappear are those
 450 which correspond to the terminal guanines (G12 and G22) and
 451 the signals of the guanines next to the terminal ones (G2 and
 452 G10) are the next to disappear. These data clearly indicate that
 453 fraying of the two last base-pairs occurs in both systems. The
 454 signals of all other imino protons disappear between 60 and
 455 70 °C in the homoduplex, but not all have disappeared at 85 °C
 456 in the heteroduplex. As the LNA:DNA duplex exhibits the
 457 higher T_m , this is not surprising. It is however difficult to try
 458 and relate these disappearance temperatures to the T_m , which
 459 characterizes the duplex as a whole and not at the individual
 460 base-pair level.

461 The imino proton exchange process at the level of an individual
 462 base-pair can be described using a two-state (open/closed) model
 463 where the imino protons are protected within the closed pair but
 464 can exchange from the transiently open pair, via an acid–base
 465 reaction catalyzed by proton acceptors (63). The formalism of
 466 catalyzed imino proton exchange from a base-pair has been
 467 extensively described in the literature and the two state model
 468 validated (54, 63). The base-pair lifetime (τ_{cl}) is equal to the imino
 469 proton exchange time if exchange occurs at each opening event,
 470 that is, in the presence of high proton acceptor concentrations.
 471 When the proton acceptor concentration is limiting, the imino
 472 proton transfer rate is function of the apparent base-pair
 473 dissociation constant, K_d , which is the ratio of the lifetimes of
 474 the open and closed states of the base-pair (τ_{op}/τ_{cl}). The plot of
 475 the proton acceptor contribution to the imino proton exchange
 476 time, $\tau_{ex,cat}$, versus the inverse of the acceptor concentration is,
 477 according to the model, a straight line whose extrapolation to
 478 infinite catalyst concentration yields the base-pair lifetime; K_d
 479 can be derived from the slope (see the Materials and Methods
 480 section) (51, 58, 63).

481 In order to extract information on the opening dynamics of a
 482 base-pair, it is necessary to integrate the signal of the imino
 483 proton which is involved in the hydrogen bond between the two
 484 complementary bases. The imino signals which are well resolved
 485 in both the DNA:DNA and in the LNA:DNA duplex are the
 486 signals of T17, G14, and G20, and these three imino protons were
 487 monitored in both systems at 15 and 25 °C. Figure 5 shows the
 488 imino proton region at 25 °C of both duplexes in the absence and
 489 in the presence of 10 mM of the proton acceptor, NH_3 . The
 490 signals broaden considerably as the catalyst concentration
 491 increases.

Table 2: Base-Pair Dissociation Constant, K_d , and Base-Pair Lifetime, τ_{cl} , of the G20, G14, and T17 Imino Protons in the DNA:DNA and LNA:DNA Duplexes at 25 °C and 15 °C

	G20	G14	T17
	K_d (10^{-6})	τ_{cl} (ms)	K_d (10^{-6})
DNA:DNA	2.42 ± 0.15	7 ± 9	2.13 ± 0.02
LNA:DNA	0.63 ± 0.02	41 ± 12	15 ± 12
	0.68 ± 0.03	35 ± 25	0.65 ± 0.05
	70 ± 34	185 ± 21	(< 8)
	0.32 ± 0.15	31 ± 3	0.32 ± 0.15
	31 ± 3	(< 4)	

“For the T17 base-pair, τ_{cl} could not be obtained from the adjustment of eq 1 to the experimental data points and the upper limit of τ_{cl} which is indicated corresponds to the $\tau_{ex,cat}$ at the highest concentration in catalyst for which the signal could still be integrated.

492 The proton acceptor contribution, $\tau_{ex,cat}$, to the imino ex-
 493 change times are shown in Figure 6 as a function of the inverse of the
 494 proton acceptor concentration. The data were fitted with a
 495 least-squares parametric adjustment to a straight line (see eq 1).
 496 The τ_{cl} and K_d obtained for each base are given in Table 2. The
 497 T17 imino signal broadens in both systems very quickly upon
 498 catalyst addition and τ_{cl} could consequently not be obtained with
 499 acceptable precision. The $\tau_{ex,cat}$ determined for the highest
 500 catalyst concentration is considered as an upper limit, but not
 501 as a good estimate, for τ_{cl} .

502 Even if the τ_{cl} of the A-T pair could not be obtained with good
 503 precision, it is clear from the comparison of the $\tau_{ex,cat}$ values
 504 (Figure 6) that in both systems the lifetime of the A-T pair is
 505 smaller than those of the G-C pairs, which is not surprising
 506 considering the more extensive hydrogen bonding of G-C
 507 base-pairs. It has been reported that in DNA:DNA duplexes, G-C
 508 base-pair lifetimes range between 5 and 50 ms and that those of
 509 A-T base-pairs range between 0.5 to 7 ms (74). The τ_{cl} of the two
 510 G-C pairs in the DNA:DNA duplex fall in the upper range of
 511 those reported in the literature and are smaller at 25 °C than at
 512 15 °C. The τ_{cl} of the two G-C pairs in the LNA:DNA hybrid
 513 duplex are larger than those of the corresponding pair in the
 514 DNA:DNA duplex and are only slightly affected by the change in
 515 temperature.

516 Base-pair lifetimes, like all kinetic parameters, do not directly
 517 provide structural information but are sensitive to local struc-
 518 ture. The study of a series of homologous RNA and DNA
 519 duplexes (54) highlights that the lifetimes of r(G-C) pairs in the

520 A-type helices tend to be longer than those of the equivalent
521 d(G-C) pairs in the B-type helices. The values obtained in this
522 study highlight that similar structural considerations could be
523 valid as the G-C base-pairs have a longer lifetime at 25 °C in the
524 A-type hybrid duplex. At 15 °C, considering the large uncertain-
525 ties on these values, it is unfortunately difficult to conclude
526 anything.

527 Regarding the dissociation constants, the K_d of the A-T base-
528 pair is, in both systems and at both temperatures, more than an
529 order of magnitude larger than the K_d of the G-C base-pairs. This
530 is consistent with data reported in the literature which highlights
531 that the G-C dissociation constants in DNA:DNA duplexes are
532 on the order of 10^{-6} and while those of A-T base-pairs are at least
533 1 order of magnitude larger (58). The substitution of cytosine
534 DNA nucleotides by their corresponding LNA equivalent in-
535 creases the stability (in other words, decreases K_d) of both the C9-
536 G14 and C3-G20 base-pairs at 25 °C. The effect is less
537 pronounced at 15 °C which is a consequence of the weaker
538 temperature dependence of the K_d values of the more stable
539 LNA:DNA pairs than of the DNA:DNA pairs. Values obtained
540 for the K_d of the C7-G16 ($0.28 \pm 0.02 \cdot 10^{-6}$ at 15 °C and $0.38 \pm$
541 $0.02 \cdot 10^{-6}$ at 25 °C) and C5-G18 ($0.29 \pm 0.02 \cdot 10^{-6}$ at 15 °C and
542 $0.35 \pm 0.02 \cdot 10^{-6}$ at 25 °C) base-pairs in the hybrid duplex display
543 the same relatively weak influence of temperature. They present a
544 slightly higher stability compared to the C9-G14 and C3-G20
545 base-pairs which could be due to their more central position in the
546 sequence. Unfortunately, no comparisons can be made with the
547 equivalent protons in the DNA:DNA duplex as their NMR
548 signals are not resolved. Concerning the K_d of the A6-T17 base-
549 pair, the substitution of the adenine DNA nucleotide by its LNA
550 equivalent has almost no effect on the dissociation constant at
551 15 °C and a destabilizing one at 25 °C. In this case, the
552 temperature has a strong influence on K_d in both systems.

553 The study of the base-pair opening dynamics of homologous
554 RNA and DNA duplexes (54) has shown that r (G-C) dissocia-
555 tion constants are smaller than d (G-C) dissociation constants
556 while r (A-U) and d (A-T) pairs exhibit comparable stabilities.
557 These results also highlight that structural features strongly
558 influence base-pair dynamics. The K_d values obtained at 15 °C
559 for the LNA:DNA duplex are similar to the values obtained for
560 RNA duplexes. Our results are furthermore coherent with the
561 results reported by McTigue et al.(34), who studied the effect of
562 the incorporation of a single LNA nucleotide on the stability of a
563 DNA duplex, and confirmed by those of You et al. (75). They
564 conclude that, even if there is an important nearest neighbor
565 dependence for each LNA base, LNA pyrimidines contribute
566 more to stability than purines. The largest stabilizing effect is
567 observed for the incorporation of a LNA cytosine and the
568 smallest for an adenine, which is also observed in this study at
569 the level of individual base-pairs. Base-pairs lifetimes have been
570 correlated to the difficulty of breaking Watson-Crick hydrogen
571 bonds and local stacking interactions (76). The increased lifetime
572 for G-C base-pairs in LNA:DNA heteroduplex correlates well
573 with the thermodynamic data reported for the LNA:DNA
574 duplex.

575 *In Summary.* We have monitored the stability and base-pair
576 dynamics of two isosequential duplexes, one composed of two
577 DNA strands the other of a full-LNA and a DNA strand. As well
578 documented in the literature, the substitution of DNA nucleo-
579 tides by LNA nucleotides increases the thermal stability of the
580 duplex and induces an A-type helical conformation. Using ITC
581 we were able to highlight that the entropic term of duplex

formation is less unfavorable for the heteroduplex than for the
582 homoduplex. The locking of the sugar in the LNA nucleotides of
583 course contributes to this $\Delta\Delta S^\circ$, but the presence of a hairpin
584 structure in the LNA single strand, highlighted by NMR and UV
585 measurements, is also favorable from this point of view. The
586 presence of this structure has however an unfavorable effect on
587 the enthalpy of duplex formation as intrastrand H-bonds must be
588 broken upon duplex formation. Taking this contribution into
589 consideration, it is possible to show that the enthalpy of forma-
590 tion of the heteroduplex from unstructured single strands would
591 be more favorable than the enthalpy of formation of the
592 homoduplex. This suggests a more efficient stacking of the bases
593 in the LNA containing duplex. The single strand structure will
594 also partially explain the large ΔC_p associated with the formation
595 of the hybrid duplex.

596 The determination by NMR magnetization transfer experi-
597 ments of individual base-pair dissociation constants provides
598 complementary information pertaining to the stability of the
599 duplexes at the level of the individual base-pairs. The substitution
600 of a cytosine by its LNA equivalent decreases the dissociation
601 constant of the G-C base-pair and increases its lifetime, while an
602 LNA substitution in an A-T base-pair does not seem to have a
603 favorable effect on its stability. A decrease in temperature does
604 not have an as important effect on the stability of a C-G base-pair
605 in the LNA:DNA duplex than in the DNA:DNA duplex. This
606 could be related to the fact that LNA nucleotides have less
607 conformational freedom, making them less sensitive to a change
608 in temperature. A more complete picture of base-pair dynamics
609 of LNA containing oligonucleotides could be helpful in the
610 design of displacement probes and primers used in hybridiza-
611 tion-based assay, where it is likely that polymerase activity is
612 dependent on the base-pair opening dynamics. The results of the
613 base-pair dynamic experiments confirm the hypothesis, reflected
614 by the more favorable ΔH° for the formation of the LNA:DNA
615 duplex from unstructured strands, that noncovalent interactions
616 in the LNA:DNA heteroduplex are more favorable than in the
617 DNA:DNA homoduplex.

618 Our conclusions are based on the comparison of the results
619 obtained for two isosequential duplexes (DNA:DNA and a full-
620 LNA:DNA) and comparison with other sequences and/or with
621 nucleotides with selective LNA substitutions would be needed in
622 order to obtain more general conclusions regarding the effect of
623 the incorporation of LNA nucleotides on the dynamics, thermo-
624 dynamics, and thermal stability of oligonucleotides. Even if much
625 work is still needed to elucidate all the factors at the origin of the
626 increase in thermodynamic and thermal stability of a duplex
627 induced by LNA substitutions, it is clear that the combined use of
628 different experimental tools (ITC, NMR, thermal denaturation
629 methods) helps to obtain a more complete picture at the
630 molecular level.

632 ACKNOWLEDGMENT

633 The authors thank Prof. Michel Luhmer for helpful discus-
634 sions pertaining to the NMR experiments and Dr. Vincent
635 Raussens for help with the CD measurements.

636 SUPPORTING INFORMATION AVAILABLE

637 ^1H NMR spectra of the imino region of the LNA single strand
638 as a function of temperature and concentration. Thermal dena-
639 turation curve of the LNA single strand monitored by UV
640 absorption spectroscopy. A table summarizing the enthalpies

641 of formation (ΔH°) determined at different temperatures by ITC
 642 for the DNA:DNA and LNA:DNA duplexes. This material is
 643 available free of charge via the Internet at <http://pubs.acs.org>.

644 REFERENCES

- 645 1. Singh, S. K., Nielsen, P., Koshkin, A. A., and Wengel, J. (1998) LNA
 646 (locked nucleic acids): synthesis and high-affinity nucleic acid recog-
 647 nition. *Chem. Commun.* 455–456.
- 648 2. Koshkin, A. A., Nielsen, P., Meldgaard, M., Rajwanshi, V. K., Singh,
 649 S. K., and Wengel, J. (1998) LNA (locked nucleic acid): an RNA
 650 mimic forming exceedingly stable LNA:LNA duplexes. *J. Am. Chem.*
 651 *Soc.* 120, 13252–13253.
- 652 3. Egli, M., Teplova, M., Minasov, G., Kumar, R., and Wengel, J. (2001)
 653 X-ray crystal structure of a locked nucleic acid (LNA) duplex
 654 composed of a palindromic 10-mer DNA strand containing one
 655 LNA thymine monomer. *Chem. Commun.* 651–652.
- 656 4. Petersen, M., and Wengel, J. (2003) LNA: a versatile tool for
 657 therapeutics and genomics. *Trends Biotechnol.* 21, 74–81.
- 658 5. Vester, B., and Wengel, J. (2004) LNA (locked nucleic acid): high-
 659 affinity targeting of complementary RNA and DNA. *Biochemistry* 43,
 660 13233–13241.
- 661 6. Jepsen, J. S., Sorensen, M. D., and Wengel, J. (2004) Locked nucleic
 662 acid: A potent nucleic acid analog in therapeutics and biotechnology.
 663 *Oligonucleotides* 14, 130–146.
- 664 7. Kaur, H., Babu, B. R., and Maiti, S. (2007) Perspectives on chemistry
 665 and therapeutic applications of locked nucleic acid (LNA). *Chem.*
 666 *Rev.* 107, 4672–4697.
- 667 8. Elmen, J., Thonberg, H., Ljungberg, K., Frieden, M., Westergaard,
 668 M., Xu, Y., Wahren, B., Liang, Z., Urum, H., Koch, T., and
 669 Wahlestedt, C. (2005) Locked nucleic acid (LNA) mediated improve-
 670 ments in siRNA stability and functionality. *Nucleic Acids Res.* 33,
 671 439–447.
- 672 9. Fluiter, K., Mook, O. R. F., and Baas, F. (2009) The therapeutic
 673 potential of LNA-modified siRNAs: reduction of off-target effects by
 674 chemical modification of the siRNA sequence. *Methods Mol. Biol.*
 675 487, 189–203.
- 676 10. Wahlestedt, C., Salmi, P., Good, L., Kela, J., Johnsson, T., Hokfelt,
 677 T., Broberger, C., Porreca, F., Lai, J., Ren, K., Ossipov, M., Koshkin,
 678 A., Jakobsen, N., Skouv, J., Oerum, H., Jacobsen, M. H., and Wengel,
 679 J. (2000) Potent and nontoxic antisense oligonucleotides containing
 680 locked nucleic acids. *Proc. Natl. Acad. Sci. U. S. A.* 97, 5633–5638.
- 681 11. Arzumanov, A., Walsh, A. P., Rajwanshi, V. K., Kumar, R., Wengel,
 682 J., and Gait, M. J. (2001) Inhibition of HIV-1 Tat-dependent trans
 683 activation by steric block chimeric 2'-O-methyl/LNA oligoribonu-
 684 cleotides. *Biochemistry* 40, 14645–14654.
- 685 12. Elayadi, A. N., Braasch, D. A., and Corey, D. R. (2002) Implications
 686 of high-affinity hybridization by locked nucleic acid oligomers for
 687 inhibition of human telomerase. *Biochemistry* 41, 9973–9981.
- 688 13. Ruiz-Ruiz, S., Moreno, P., Guerri, J., and Ambros, S. (2009)
 689 Discrimination between mild and severe Citrus tristeza virus isolates
 690 with a rapid and highly specific real-time reverse transcription-poly-
 691 merase chain reaction method using TaqMan LNA probes. *Phyto-*
 692 *pathology* 99, 307–315.
- 693 14. Stenvang, J., Lindow, M., and Kauppinen, S. (2008) Targeting of
 694 microRNAs for therapeutics. *Biochem. Soc. Trans.* 36, 1197–1200.
- 695 15. Beane, R., Gabillet, S., Montaillier, C., Arar, K., and Corey, D. R.
 696 (2008) Recognition of chromosomal DNA inside cells by locked
 697 nucleic acids. *Biochemistry* 47, 13147–13149.
- 698 16. Veedu, R. N., Vester, B., and Wengel, J. (2008) Polymerase chain
 699 reaction and transcription using locked nucleic acid nucleotide
 700 triphosphates. *J. Am. Chem. Soc.* 130, 8124–8125.
- 701 17. Yamada, K., Terahara, T., Kurata, S., Yokomaku, T., Tsuneda, S.,
 702 and Harayama, S. (2008) Retrieval of entire genes from environmen-
 703 tal DNA by inverse PCR with pre-amplification of target genes using
 704 primers containing locked nucleic acids. *Environ. Microbiol.* 10, 978–
 705 987.
- 706 18. Ballantyne, K. N., van Oorschot, R. A. H., and Mitchell, R. J. (2008)
 707 Locked nucleic acids in PCR primers increase sensitivity and perfor-
 708 mance. *Genomics* 91, 301–305.
- 709 19. Gustafson, K. S. (2008) Locked nucleic acids can enhance the
 710 analytical performance of quantitative methylation-specific polymer-
 711 ase chain reaction. *J. Mol. Diagn.* 10, 33–42.
- 712 20. Kurreck, J., Wyszko, E., Gillen, C., and Erdmann, V. A. (2002)
 713 Design of antisense oligonucleotides stabilized by locked nucleic
 714 acids. *Nucleic Acids Res.* 30, 1911–1918.
- 715 21. Petersen, M., Nielsen, C. B., Nielsen, K. E., Jensen, G. A., Bondensgaard,
 716 K., Singh, S. K., Rajwanshi, V. K., Koshkin, A. A., Dahl, B. M., Wengel,
 J., and Jacobsen, J. P. (2000) The conformations of locked nucleic acids
 (LNA). *J. Mol. Recognit.* 13, 44–53.
- 717 22. Petersen, M., Bondensgaard, K., Wengel, J., and Jacobsen, J. P.
 718 (2002) Locked nucleic acid (LNA) recognition of RNA: NMR
 719 solution structures of LNA:RNA hybrids. *J. Am. Chem. Soc.* 124,
 720 5974–5982.
- 721 23. Nielsen, K. E., Singh, S. K., Wengel, J., and Jacobsen, J. P. (2000)
 722 Solution structure of an LNA hybridized to DNA: NMR study of the
 723 d(CTLGCTLTLCTLGC):d(CGAGAAGCAG) duplex containing
 724 four locked nucleotides. *Bioconjug. Chem.* 11, 228–238.
- 725 24. Nielsen, K. E., Rasmussen, J., Kumar, R., Wengel, J., Jacobsen, J. P.,
 726 and Petersen, M. (2004) NMR studies of fully modified locked nucleic
 727 acid (LNA) hybrids: solution structure of an LNA:RNA hybrid and
 728 characterization of an LNA:DNA hybrid. *Bioconjug. Chem.* 15, 449–
 729 457.
- 730 25. Nielsen, C. B., Singh, S. K., Wengel, J., and Jacobsen, J. P. (1999) The
 731 solution structure of a locked nucleic acid (LNA) hybridized to DNA.
 732 *J. Biomol. Struct. Dyn.* 17, 175–191.
- 733 26. Bondensgaard, K., Petersen, M., Singh, S. K., Rajwanshi, V. K.,
 734 Kumar, R., Wengel, J., and Jacobsen, J. P. (2000) Structural studies of
 735 LNA:RNA duplexes by NMR: conformations and implications for
 736 RNase H activity. *Chem.-Eur. J.* 6, 2687–2695.
- 737 27. Ivanova, A., and Roesch, N. (2007) The structure of LNA:DNA
 738 hybrids from molecular dynamics simulations: the effect of locked
 739 nucleotides. *J. Phys. Chem. A* 111, 9307–9319.
- 740 28. Pande, V., and Nilsson, L. (2008) Insights into structure, dynamics
 741 and hydration of locked nucleic acid (LNA) strand-based duplexes
 742 from molecular dynamics simulations. *Nucleic Acids Res.* 36, 1508–
 743 1516.
- 744 29. Obika, S., Nanbu, D., Hari, Y., Andoh, J.-I., Morio, K.-I., Doi, T.,
 745 and Imanishi, T. (1998) Stability and structural features of the
 746 duplexes containing nucleoside analogs with a fixed N-type confor-
 747 mation. 2'-O,4'-C-methylenerybonucleosides. *Tetrahedron Lett.* 39,
 748 5401–5404.
- 749 30. Koshkin, A. A., Singh, S. K., Nielsen, P., Rajwanshi, V. K., Kumar,
 750 R., Meldgaard, M., Olsen, C. E., and Wengel, J. (1998) LNA (locked
 751 nucleic acids): synthesis of the adenine, cytosine, guanine, 5-methyl-
 752 cytosine, thymine and uracil bicyclonucleoside monomers, oligomer-
 753 ization, and unprecedented nucleic acid recognition. *Tetrahedron* 54,
 754 3607–3630.
- 755 31. Singh, S. K., and Wengel, J. (1998) Universality of LNA-mediated
 756 high-affinity nucleic acid recognition. *Chem. Commun.* 1247–1248.
- 757 32. Orum, H., Jakobsen, M. H., Koch, T., Vuust, J., and Borre, M. B.
 758 (1999) Detection of the factor V Leiden mutation by direct allele-
 759 specific hybridization of PCR amplicons to photoimmobilized locked
 760 nucleic acids. *Clin. Chem.* 45, 1898–1905.
- 761 33. Braasch, D. A., and Corey, D. R. (2001) Locked nucleic acid (LNA):
 762 fine-tuning the recognition of DNA and RNA. *Chem. Biol.* 8, 1–7.
- 763 34. McTigue, P. M., Peterson, R. J., and Kahn, J. D. (2004) Sequence-
 764 dependent thermodynamic parameters for locked nucleic acid (LNA)-
 765 DNA duplex formation. *Biochemistry* 43, 5388–5405.
- 766 35. Kaur, H., Arora, A., Wengel, J., and Maiti, S. (2006) Thermody-
 767 namic, counterion, and hydration effects for the incorporation of
 768 locked nucleic acid nucleotides into DNA duplexes. *Biochemistry* 45,
 769 7347–7355.
- 770 36. Kaur, H., Wengel, J., and Maiti, S. (2008) Thermodynamics of DNA-
 771 RNA heteroduplex formation: effects of locked nucleic acid nucleo-
 772 tides incorporated into the DNA strand. *Biochemistry* 47, 1218–1227.
- 773 37. Christensen, U., Jacobsen, N., Rajwanshi, V. K., Wengel, J., and
 774 Koch, T. (2001) Stopped-flow kinetics of locked nucleic acid (LNA)-
 775 oligonucleotide duplex formation: studies of LNA-DNA and DNA-
 776 DNA interactions. *Biochem. J.* 354, 481–484.
- 777 38. Christensen, U. (2007) Thermodynamic and kinetic characterization
 778 of duplex formation between 2'-O, 4'-C-methylene-modified oligo-
 779 ribonucleotides, DNA and RNA. *Biosci. Rep.* 27, 327–333.
- 780 39. Kierzek, E., Pasternak, A., Pasternak, K., Gdaniec, Z., Yildirim, I.,
 781 Turner, D. H., and Kierzek, R. (2009) Contributions of stacking,
 782 preorganization, and hydrogen bonding to the thermodynamic sta-
 783 bility of duplexes between RNA and 2'-O-methyl RNA with locked
 784 nucleic acids. *Biochemistry* 48, 4377–4387.
- 785 40. Kierzek, E., Ciesielska, A., Pasternak, K., Mathews, D. H., Turner,
 786 D. H., and Kierzek, R. (2005) The influence of locked nucleic acid
 787 residues on the thermodynamic properties of 2'-O-methyl RNA/RNA
 788 heteroduplexes. *Nucleic Acids Res.* 33, 5082–5093.
- 789 41. Tikhomirova, A., Taulier, N., and Chalikian, T. V. (2004) Energetics
 790 of nucleic acid stability: the effect of Δ CP. *J. Am. Chem. Soc.* 126,
 791 16387–16394.
- 792 42. Mikulecky, P. J., and Feig, A. L. (2006) Heat capacity changes
 793 associated with nucleic acid folding. *Biopolymers* 82, 38–58.
- 794 795

- 796 43. Feig, A. L. (2007) Applications of isothermal titration calorimetry in
797 RNA biochemistry and biophysics. *Biopolymers* 87, 293–301. 850
- 798 44. Jelesarov, I., Crane-Robinson, C., and Privalov, P. L. (1999) The
799 energetics of HMG box interactions with DNA: thermodynamic
800 description of the target DNA duplexes. *J. Mol. Biol.* 294, 981–995. 851
- 801 45. Takach, J. C., Mikulecky, P. J., and Feig, A. L. (2004) Salt-dependent
802 heat capacity changes for RNA duplex formation. *J. Am. Chem. Soc.*
803 *126*, 6530–6531. 852
- 804 46. Mikulecky, P. J., and Feig, A. L. (2006) Heat capacity changes
805 associated with DNA duplex formation: salt- and sequence-dependent
806 effects. *Biochemistry* 45, 604–616. 853
- 807 47. Lang, B. E., and Schwarz, F. P. (2007) Thermodynamic dependence of
808 DNA/DNA and DNA/RNA hybridization reactions on temperature
809 and ionic strength. *Biophys. Chem.* 131, 96–104. 854
- 810 48. Holbrook, J. A., Capp, M. W., Saecker, R. M., and Record, M. T. Jr.
811 (1999) Enthalpy and heat capacity changes for formation of an
812 oligomeric DNA duplex: interpretation in terms of coupled processes
813 of formation and association of single-stranded helices. *Biochemistry*
814 *38*, 8409–8422. 855
- 815 49. Jourdan, M. (1998) Ph.D. Thesis, Université Joseph Fourier, Greno-
816 ble, France. 856
- 817 50. Cahen, P., Luhmer, M., Fontaine, C., Morat, C., Reisse, J., and
818 Bartik, K. (2000) Study by ²³Na-NMR, ¹H-NMR, and ultraviolet
819 spectroscopy of the thermal stability of an 11-basepair oligonucleo-
820 tide. *Biophys. J.* 78, 1059–1069. 857
- 821 51. Leroy, J. L., Kochoyan, M., Huynh Dinh, T., and Gueron, M. (1988)
822 Characterization of base-pair opening in deoxynucleotide duplexes
823 using catalyzed exchange of the imino proton. *J. Mol. Biol.* 200, 223–
824 238. 858
- 825 52. Leroy, J. L., Charretier, E., Kochoyan, M., and Gueron, M. (1988)
826 Evidence from base-pair kinetics for two types of adenine tract
827 structures in solution: their relation to DNA curvature. *Biochemistry*
828 *27*, 8894–8898. 859
- 829 53. Kochoyan, M., Leroy, J. L., and Gueron, M. (1990) Processes of base-
830 pair opening and proton exchange in Z-DNA. *Biochemistry* 29, 4799–
831 4805. 860
- 832 54. Snoussi, K., and Leroy, J. L. (2002) Alteration of A•T base-pair
833 opening kinetics by the ammonium cation in DNA A-tracts. *Bio-*
834 *chemistry* 41, 12467–12474. 861
- 835 55. Varnai, P., Canalia, M., and Leroy, J.-L. (2004) Opening mechanism
836 of G•T/U pairs in DNA and RNA duplexes: a combined study of
837 imino proton exchange and molecular dynamics simulation. *J. Am.*
838 *Chem. Soc.* 126, 14659–14667. 862
- 839 56. Leroy, J. L., Gao, X. L., Misra, V., Gueron, M., and Patel, D. J. (1992)
840 Proton exchange in DNA-luzopeptin and DNA-echinomycin bisin-
841 tercalation complexes: rates and processes of base-pair opening.
842 *Biochemistry* 31, 1407–1415. 863
- 843 57. Leroy, J. L., Bolo, N., Figueroa, N., Plateau, P., and Gueron, M.
844 (1985) Internal motions of transfer RNA: a study of exchanging
845 protons by magnetic resonance. *J. Biomol. Struct. Dyn.* 2, 915–939. 864
- 846 58. Snoussi, K., and Leroy, J. L. (2001) Imino Proton Exchange and Base-
847 Pair Kinetics in RNA Duplexes. *Biochemistry* 40, 8898–8904. 865
- 848 59. Cahen, P. (2000) Ph.D. Thesis, Université Libre de Bruxelles,
849 Brussels, Belgium. 866
60. Fasman, G. D. (1975) Handbook of Biochemistry and Molecular
Biology, Vol. 1: Nucleic Acids., 3rd ed., CRC Press, Cleveland, OH. 867
61. Petersheim, M., and Turner, D. H. (1983) Base-stacking and base-
pairing contributions to helix stability: thermodynamics of double-
helix formation with CCGG, CCGGp, CCGGAp, ACCGGp,
CCGGUp, and ACCGGUp. *Biochemistry* 22, 256–263. 868
62. Plateau, P., and Gueron, M. (1982) Exchangeable proton NMR
without base-line distortion, using new strong-pulse sequences.
J. Am. Chem. Soc. 104, 7310–7311. 869
63. Gueron, M., and Leroy, J.-L. (1995) Studies of base pair kinetics by
NMR measurement of proton exchange. *Methods Enzymol.* 261, 383–
413. 870
64. Phan, A. T., Gueron, M., and Leroy, J. L. (2001) Investigation of
unusual DNA motifs. *Methods Enzymol.* 338, 341–371. 871
65. Schmidt, K. S., Borkowski, S., Kurreck, J., Stephens, A. W., Bald,
R., Hecht, M., Friebe, M., Dinkelborg, L., and Erdmann, V. A.
(2004) Application of locked nucleic acids to improve aptamer in
vivo stability and targeting function. *Nucleic Acids Res.* 32, 5757–
5765. 872
66. Vesnaver, G., and Breslauer, K. J. (1991) The contribution of DNA
single-stranded order to the thermodynamics of duplex formation.
Proc. Natl. Acad. Sci. U. S. A. 88, 3569–3573. 873
67. Searle, M. S., and Williams, D. H. (1993) On the stability of nucleic
acid structures in solution: Enthalpy-entropy compensations, internal
rotations and reversibility. *Nucleic Acids Res.* 21, 2051–2056. 874
68. Bloomfield, V. A., Crothers, D. M. Tinoco, I., Jr. (2000) Nucleic
Acids: Structures, Properties, and Functions, University Science Books,
Sausalito, CA. 875
69. Mirau, P. A., and Kearns, D. R. (1984) Effect of environment,
conformation, sequence and base substituents on the imino proton
exchange rates in guanine and inosine-containing DNA, RNA, and
DNA-RNA duplexes. *J. Mol. Biol.* 177, 207–227. 876
70. Wu, P., Nakano, S.-I., and Sugimoto, N. (2002) Temperature depen-
dence of thermodynamic properties for DNA/DNA and RNA/DNA
duplex formation. *Eur. J. Biochem.* 269, 2821–2830. 877
71. Patel, D. J., Ikuta, S., Kozlowski, S., and Itakura, K. (1983) Sequence
dependence of hydrogen exchange kinetics in DNA duplexes at the
individual base pair level in solution. *Proc. Natl. Acad. Sci. U. S. A.* 80,
2184–2188. 878
72. Leijon, M., and Graeslund, A. (1992) Effects of sequence and length
on imino proton exchange and base pair opening kinetics in DNA
oligonucleotide duplexes. *Nucleic Acids Res.* 20, 5339–5343. 879
73. Dornberger, U., Leijon, M., and Fritzsche, H. (1999) High base pair
opening rates in tracts of GC base pairs. *J. Biol. Chem.* 274, 6957–
6962. 880
74. Gueron, M. Leroy, J. L. (1992) Base-pair opening in double-stranded
nucleic acids, in Nucleic Acids Mol. Biol. (Eckstein, F., Lilley, D. M. J.,
Eds.) pp 1–22, Springer-Verlag, Berlin. 881
75. You, Y., Moreira, B. G., Behlke, M. A., and Owczarzy, R. (2006)
Design of LNA probes that improve mismatch discrimination.
Nucleic Acids Res. 34, e60/1–e60/11. 882
76. Giudice, E., and Lavery, R. (2003) Nucleic acid base pair dynamics:
the impact of sequence and structure using free-energy calculations.
J. Am. Chem. Soc. 125, 4998–4999. 883